4464–4473 *Nucleic Acids Research, 1997, Vol. 25, No. 22*

Functional recognition of fragmented operator sites by R17/MS2 coat protein, a translational repressor

Derrick E. Fouts[+], Heather L. True and Daniel W. Celander[1,*]

Department of Microbiology and [1]College of Medicine, University of Illinois at Urbana-Champaign, B103 Chemical and Life Sciences Laboratory, 601 South Goodwin Avenue, Urbana, IL 61801, USA

Received August 22, 1997; Revised and Accepted October 7, 1997

ABSTRACT

The R17/MS2 coat protein serves as a translational repressor of replicase by binding to a 19 nt RNA hairpin containing the Shine–Dalgarno sequence and the initiation codon of the replicase gene. We have explored the structural features of the RNA operator site that are necessary for efficient translational repression by the R17/MS2 coat protein *in vivo*. The R17/MS2 coat protein efficiently directs lysogen formation for P22$_{R17}$, a bacteriophage P22 derivative that carries the R17/MS2 RNA operator site within the P22 phage *ant* mRNA. Phages were constructed that contain fragmented operator sites such that the Shine–Dalgarno sequence and the initiation codon of the affected gene are not located within the RNA hairpin. The wild-type coat protein directs efficient lysogen formation for P22 phages that carry several fragmented RNA operator sites, including one in which the Shine–Dalgarno sequence is positioned 4 nt outside the coat protein binding site. Neither the wild-type R17/MS2 coat protein nor super-repressor mutants induce lysogen formation for a P22 phage encoding an RNA hairpin at a distance of 9 nt from the Shine–Dalgarno sequence, implying that a discrete region of biological repression is defined by the coat protein–RNA hairpin interaction. The assembly of RNA species into capsid structures is not an efficient means whereby the coat protein achieves translational repression of target mRNA transcripts. The R17/MS2 coat protein exerts translational regulation that extends considerably beyond the natural biological RNA operator site structure; however, the coat protein still mediates repression in these constructs by preventing ribosome access to linear sequence determinants of the translational initiation region by the formation of a stable RNA secondary structure. An efficient translational regulatory mechanism in bacteria appears to reside in the ability of proteins to regulate RNA folding states for host cell and phage mRNAs.

INTRODUCTION

RNA-binding proteins can initiate translational repression by a variety of mechanisms. Most examples of translational regulation in prokaryotes focus on perturbing the formation of a functional initiation complex (1). The R17/MS2 coat protein causes translational repression by binding to an RNA secondary structure within the translational initiation region of the coliphage replicase gene (2). The most widely accepted model for translational repression by the coat protein suggests that the prevention of binary complex formation occurs by sequestering the Shine–Dalgarno sequence and initiation codon in secondary structure (1,3,4). Coat protein binding to the RNA stabilizes the secondary structure and prevents ribosomal access to the Shine–Dalgarno sequence (3). Another model proposes that the coat protein occludes access to the RNA by physically masking the Shine–Dalgarno sequence and the initiation codon (1). The latter model does not invoke a specific conformation that the RNA target sequence must adopt for translational regulation. These models are not mutually exclusive and are difficult to differentiate because sequestration and occlusion occur simultaneously in the natural R17/MS2 replicase operator site.

We have applied the RNA challenge phage system as a genetic tool (5) to evaluate different types of R17/MS2 coat protein binding site structures as translational operator sites. Our objective with these studies was to evaluate whether sequestration or occlusion represents the predominant mechanism for early translational regulation of an artificial operator site by the R17/MS2 coat protein. Our findings reveal that the coat protein can exert translational regulation well outside the confines of its RNA binding site.

Coat proteins may also direct translational repression late in the infection by drawing RNA transcripts into capsid assemblies. This mode of translational regulation has not been studied extensively in the context of the native R17/MS2 phage life cycle, but it would be amenable to investigation using heterologous reporter systems (6,7). Further insights into the capsid's role in translational repression were obtained through our comparative studies of the effectiveness in which coat proteins encoding different types of defects in capsid assembly can functionally recognize artificial operator sites.

MATERIALS AND METHODS

Standard reagents

Biochemical reagents were of the highest grade obtainable from various manufacturers. Sterile water was initially deionized using a Millipore Milli-Q Plus water purification system. The

*To whom correspondence should be addressed. Tel: +1 217 244 6433; Fax: +1 217 244 6433; Email: dcelande@uiuc.edu

[+]Present address: Department of Plant Pathology, Cornell University, Ithaca, NY 14853-0001, USA

oligonucleotides were purchased from Operon Technologies, Inc. The [γ-^{32}P]ATP (6000 Ci/mmol) was obtained from DuPont-New England Nuclear. Horseradish peroxidase coupled goat anti-rabbit IgG antibody was purchased from Zymed Laboratories, Inc. The chemiluminescence reagents were obtained from Amersham, Inc. and DuPont-NEN. Enzymes were obtained from New England Biolabs.

Oligonucleotides and site-directed mutagenesis

The following molecules were used in this study: L12: 5′-GGCTTCGGTTGTCAGTAGATCTAGTTCCATCATTAGAGGAACCAACATGAATAGTATAG-3′; L14: 5′-GGCTTCGGTTGTCAGTAGATCTGATCCTCATGATTACAGAGGAACCAACATGAATAGTATAGC-3′; L18: 5′-GGCTTCGGTTGTCAGTAGATCTGACGTAGATGATTACACTACGAGGAACCAACATGAATAGTATAG-3′; L18/19: 5′-GGCTTCGGTTGTCAGTAGATCTGACGTACAGCATTAGCGTACGAGGAACCAACATGAATAGTATAG-3′; L19: 5′-GGCTTGGTTGTCAGATCTACAGCATTAGCGTAGAGAGGAACCAACATGAATAG-3′; L23: 5′-CAGGGCTTCGGTTGTCAGATCTACAGCATTAGCGTAGACTTTGAGGAACCAACATGAATAGTATAG-3′; L28: 5′-CAGGGCTTCGGTTGTCATCTACAGCATTAGCGTAGACAGATCTTTGAGGAACCAACATGAATAGTATAG-3′; Anti-Omnt: 5′-GATCATCTCTAGCCATGC-3′: Intra-Ant: 5′-GCGGTAAGAACATGCTGTC-3′; and Arc-Ant: 5′-CCAACTGCGGTAACAGTCAG-3′. The DNA sequences that encode the modified RNA target sites were incorporated into either pMMW20 or pΦGen1 according to standard procedures (9) using a single-stranded phagemid DNA template of either pMMW20 (5) or pΦGen1 (8) that contained deoxyuridine residues and DNA oligonucleotides L12, L14, L18, L18/19, L19, L23 and L28.

PCR–RFLP analysis

Bacteriophage or plasmid DNA served as the template for amplification reactions. PCR assays were done with phage suspension (~10^8 p.f.u.) or plasmid DNA (~10^8 molecules) in the presence of 0.4 μM each of Anti-Omnt and Intra-Ant primers, 0.5 Unit Vent$_R$™ DNA Polymerase, 0.1 mM dNTPs in 10 mM KCl, 20 mM Tris–HCl (pH 8.8 at 25°C), 10 mM $(NH_4)_2SO_4$, 2 mM $MgSO_4$ and 0.1% Triton X-100. The PCR products (10 μl of a 100 μl PCR reaction) were subsequently digested with restriction endonucleases (0.25–1 U/μl) for 1 h according to the manufacturer's instructions.

Analysis of PCR products by dideoxynucleotide cycle sequencing

The buffer components were separated from the amplified DNA products using diafiltration in a 30 000 NMWL Ultra Free-MC ultrafiltration unit (Millipore, Inc.) according to the manufacturer's instructions. The retentate containing the DNA was exchanged into TE buffer (10 mM Tris–HCl, pH 8.0, 1 mM EDTA) and adjusted to a final volume of 20 μl. Chain-termination sequencing reactions were performed with the PCR products (3 μl) using 5′-^{32}P-labeled Intra-Ant and Arc-Ant primers and the cycle sequencing procedure as originally described (10).

Bacteriological reagents and methods

The genotypes of the bacteriological reagents used in this work are illustrated in Table 1. The P22 bacteriophages that encode a consensus operator site or a fragmented operator site in the 5′-end of the *ant* gene were constructed by homologous recombination in *Salmonella typhimurium* strain MS1883 as summarized in Figure 1c. In the original construction method (5), the DNA sequence encoding the desired RNA operator site was introduced into the P22 *immI* (*arc*$^+$) region of pMMW20 using site-directed mutagenesis. An MS1883 transformant containing the resultant plasmid derivative was then infected with P22*mnt*::Kn9*arc*(Am) to allow for homologous recombination between the resident plasmid and the infecting bacteriophage. Dilutions of the resultant phage lysate were plated on a lawn of MS1582 cells to permit the identification of turbid phage plaques that contain the recombinant *arc* allele. The *arc*$^+$ phages that encode the RNA hairpin were identified by PCR–RFLP and direct sequence analyses. The *arc*(Am) allele was re-introduced into the resultant P22 phage derivative by performing a mixed infection with the phage encoding the RNA hairpin and a replication-defective helper phage derivative containing the *arc*(Am) allele [P22*mnt*::Kn9O$_{mnt}$::*Sma*I–*Eco*RI-*arcH1605*(Am)*ant::lacZ*] in MS1883. Phage lysates produced from the infection were plated on a lawn of MS1883 cells to permit identification of the clear phage plaques that contain the *arc*(Am) allele. The presence of the *arc*(Am) allele and the integrity of the encoded RNA hairpin in the final phage derivative were confirmed using PCR/RFLP and DNA sequence analyses.

In the revised construction method (8), the DNA sequence encoding the desired RNA hairpin was introduced into the P22 *immI* [*arc*(Am)] region of pΦGen1 using site-directed mutagenesis. An MS1883 transformant containing the resultant plasmid derivative was then infected with P22*mnt*::Kn9 to allow for homologous recombination between the resident plasmid and the infecting bacteriophage. Dilutions of the resultant phage lysate were plated on a lawn of MS1582 cells to permit the identification of clear phage plaques that contain the recombinant *arc*(Am) allele. The presence of the *arc*(Am) allele and integrity of the DNA sequence encoding the RNA hairpin was verified by PCR/RFLP analyses of the *immI* region and DNA sequence analyses of the 5′ end of the *ant* gene using the cycle sequencing procedure with Vent (exo$^-$) DNA polymerase (10).

The plasmids pR17coat(+)[N55K] and pR17coat(+)[A1D/N55K] were identified from a library of coat gene mutants that could promote lysogen formation for P22$_{R17}$[A(–10)U] using a genetic selection scheme described previously (11). The coding sequence that corresponds to the R17/MS2 coat protein mutant [A1D] was originally isolated from a pR17coat(+)ΔS plasmid library. The plasmid pR17coat(+)[A1D] was constructed by removing the coat gene from pR17coat(+)ΔS[A1D] using *Xba*I and *Hin*dIII restriction endonucleases and inserting the gene into pR17coat(+)-1.13 vector. Plasmid DNAs and bacteriophages were introduced into the *S.typhimurium* strains as described previously (5).

RNA challenge phage assays

Briefly, MS1868 transformants containing one of the R17/MS2 coat protein expression plasmids were cultured to a cell density of ~5×10^8 cells/ml in LB media supplemented with ampicillin (100 μg/ml). MS1868 recipients (5×10^7 cells) were inoculated with the appropriate P22 challenge phage at a multiplicity of infection of 10–20. Following phage adsorption at 20°C for 20 min, the infected

cells were plated onto LB-agar plates containing the appropriate antibiotics. The number of lysogens that formed was determined by plating an appropriate serial dilution of infected cells on LB plates containing ampicillin (100 μg/ml) and kanamycin (50 μg/ml). Viable cell counts were determined in a similar fashion by plating uninfected cells on LB agar plates supplemented with ampicillin (100 μg/ml). The frequency of lysogenization (expressed as % lysogeny) was calculated as the number of colonies obtained on the LB plates containing ampicillin and kanamycin divided by the number of viable colonies obtained on the LB plates containing ampicillin, multiplied by 100.

Biochemical and immunological methods

The SDS–polyacrylamide gel electrophoresis experiments (SDS–PAGE) were carried out as described (11). The gels were fixed and stained with either silver nitrate or FastStain (Zoion, Inc.) according to the manufacturer's instructions. Immunoblots were prepared by electrophoretic transfer of proteins from SDS–PAGE gels onto Immobilon PVDF membranes (Millipore Corp.). Membrane-bound coat proteins were detected with a rabbit anti-R17 coat protein polyclonal antiserum and visualized using a horseradish peroxidase linked goat anti-rabbit IgG (Zymed Laboratories, Inc.) with either an ECL Western detection kit (Amersham, Inc.) or the 3,3′-diaminobenzidine/H_2O_2/$NiCl_2$ detection system (11).

MS1868 cultures (3 ml) that express a given coat protein were grown at 37°C to an OD_{600} of ~0.6, and the coat protein expression was induced by adding IPTG to a final concentration of 1 mM for 1 h. The cells were harvested by centrifugation at 12 000 *g* at 4°C for 3 min. Each cell pellet was resuspended in 0.3 ml of NGE buffer (0.05 M NaH_2PO_4, pH 7.0, 0.001 M $MgCl_2$) and sonicated on ice. The cell lysates were clarified by centrifugation at 12 000 *g* at 4°C for 10 min. An aliquot of each lysate was adjusted to contain 1× loading buffer (5% glycerol, 0.04% xylene cyanole and 0.04% bromophenol blue) and subjected to electrophoresis (0.8 V/cm) in 0.9% agarose gels with circulating NGE buffer at room temperature until the bromophenol blue migrated ~7 cm. The proteins were then transferred to a nitrocellulose membrane (MSI) by capillary blotting using NGE buffer before immunoblot analysis.

Table 1. Biological reagents used

Biological reagent	Relevant characteristics	Source or ref.
Strain		
Escherichia coli		
CJ236	F′ [pCJ105 (Cm^R)] *dut-1 ung-1 thi-1 relA1*	9
XL1-Blue	*recA1 endA1 gyrA96 thi-1 hsdR17 supE44*	
	relA1 lac [F′ *proAB lacI*^{q}ZΔ*M15* Tn*10* (Tc^R)]	43
DH5α	F^-, Φ80d*lacZ*Δ*M15*, *recA1*, *endA1*, *gyrA96*,	
	thi-1, *hsdR17* (r_k^-, m_k^+), *supE44*, *relA1*,	
	deoR, Δ(*lacZYA-argF*)U169	D. Hanahan
Salmonella typhimurium		
MS1582	LT2 *leuA414*(Am) $Fels^-$ *supE40*	
	ataP::[P22 *sieA44* 16(Am)*H1455* Tpfr49]	M. Susskind
MS1883	LT2 *leuA414* $Fels^-$ *hsdSB* (r^-m^+) *supE40*	M. Susskind
MS1868	LT2 *leuA414(Am)* $Fels^-$ *hsdSB* (r^-m^+) *endE40*	M. Susskind
Bacteriophage		
P22*mnt*::Kn9*arc*(Am)	O_{mnt}^+ *arc*(Am)	5
P22*mnt*::Kn9O_{mnt}::*Sma*I–*Eco*RI		
arcH1605(Am)*ant::lacZ*	O_{mnt}::*Sma*I–*Eco*RI *arc*(Am) *ant::lacZ*	5
P22*mnt*::Kn9	O_{mnt}^+ *arc*$^+$	8
$P22_{R17}$	P22*mnt*::Kn9 O_{mnt}::*Sma*I–*Eco*RI *arc*(Am)	
	O^+_{R17} replicase::*ant*	5
$P22_{R17}$[A(–10)U]	P22*mnt*::Kn9 O_{mnt}::*Sma*I–*Eco*RI *arc*(Am)	
	O^c_{R17} replicase::*ant*	5
Plasmid		
pCKR101	pBR322 *lacI*^{q} P_{tac} polylinker	R. Dahlquist
pMMW20	pPY190 O_{mnt}::*Sma*I–*Eco*RI *arc*$^+$ *ant*′	5
pΦGen1	pPY190 *mnt*::Kn9 O_{mnt}::*Sma*I–*Eco*RI *arc*(Am) *ant*′	8
pR17coat(+)	pCKR101, R17 coat gene (sense orientation)	
	~465 bp of 5′-untranslated leader sequence	5
pR17coat(+)-1.13	pR17coat(+), coat gene insert flanked by unique	
	*Xba*I and *Hin*dIII restriction endonuclease sites	11
pR17coat(+)[A1D]	pR17coat(+) with codon 1 substitution mutation	11
pR17coat(+)[N55K]	pR17coat(+) with codon 55 substitution mutation	11
pR17coat(+)[A1D/N55K]	pR17coat(+)-1.13 with codons 1 and 55	
	substitution mutations	this work

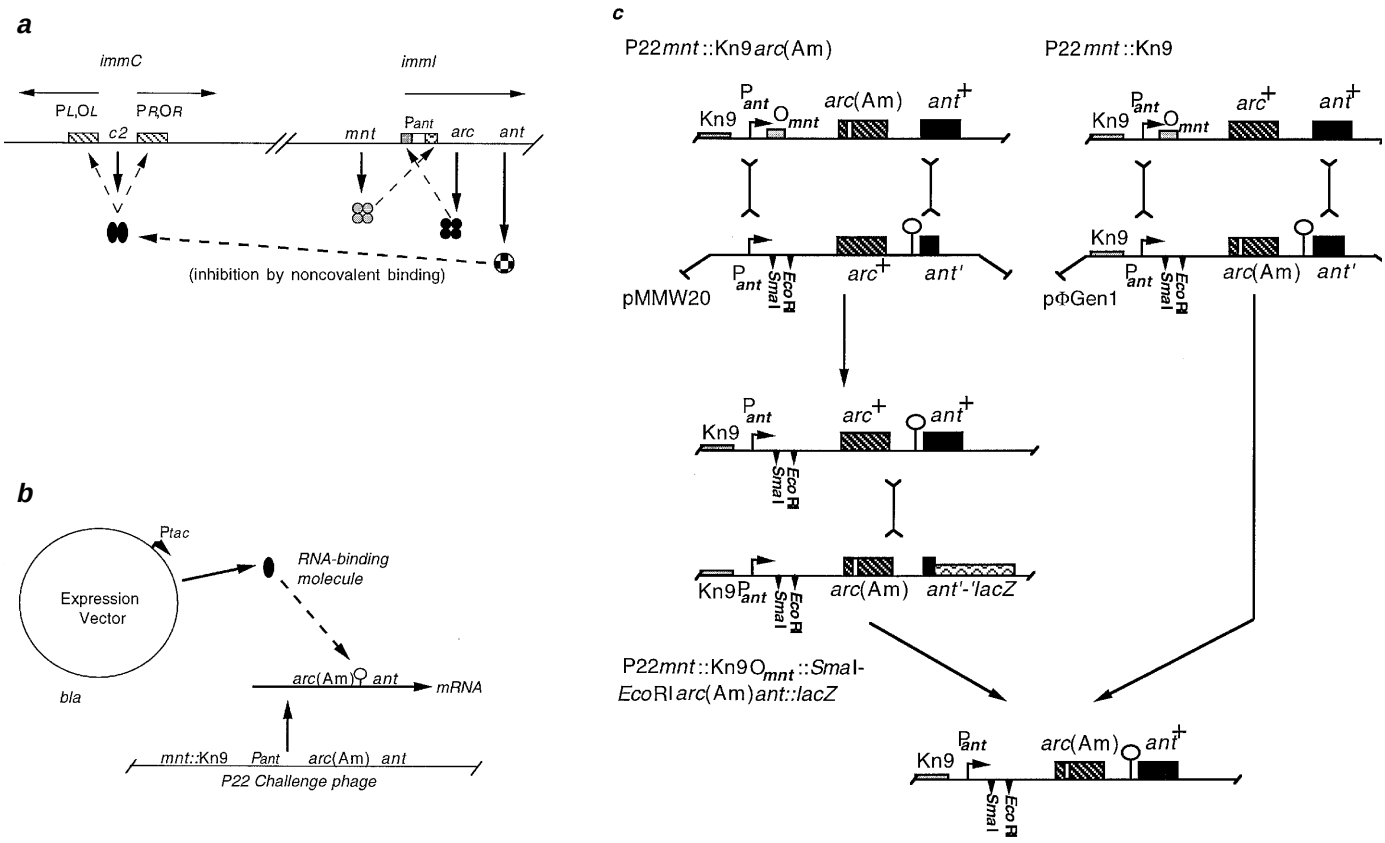

Figure 1. (**a**) Life cycle of bacteriophage P22. Solid lines refer to expression of regulatory gene products. Dashed lines refer to negative regulatory pathways. For a more detailed discussion, see the description in the text. (**b**) RNA challenge phage development. The modified P22 phage contains an amber mutation in *arc* [*arc*(Am)] and a kanamycin resistance cassette inserted into the *mnt* gene (*mnt*::Kn9). The region encoding the ribosome binding site of the *ant* gene is substituted by a sequence encoding an RNA sequence (shown by the lollipop) recognized by an RNA-binding molecule. The RNA binding molecule is produced from an expression vector. The relative amounts of c2 and Ant proteins synthesized in an infected cell will dictate whether the phage becomes a lysogen or undergoes lytic growth. If a sufficient amount of the RNA binding molecule is present in the cell, it will saturate its specific RNA binding site on the newly synthesized *ant* mRNA transcripts following infection and inhibit Ant translation. Repression of Ant synthesis allows c2-mediated establishment of lysogeny. This results in the formation of a kanamycin-resistant lysogen. Lysogenic development of each phage that is described in this study relies upon expression of the R17/MS2 coat protein in the susceptible host cell and the availability of a suitable RNA-binding site encoded by each phage genome. (**c**) RNA challenge phage construction. The original method is outlined on the left panel. The revised method is illustrated on the right panel (see Materials and Methods for details).

RESULTS

Previously, we described the use of a temperate DNA bacteriophage P22 derivative to evaluate RNA–protein interactions within a biological context (5). Two sets of genes normally determine the developmental fate of bacteriophage P22 in an infected *S.typhimurium* host cell (Fig. 1a). These genes reside in two genetically distinct loci within the bacteriophage genome termed the immunity regions, *immC* and *immI*. The expression of the *c2* gene product, which resides in *immC*, causes the bacteriophage to establish and maintain a dormant, lysogenic state in the infected host cell. The c2 protein represses lytic gene functions by binding to two DNA operator regions (12). The *immI* region contains two additional repressor proteins termed Mnt and Arc, and an antirepressor protein called Ant. Expression of these genes occurs from two divergently transcribed operons. One transcription unit consists of P_{mnt} and the *mnt* gene. The second unit consists of P_{ant} and the *arc* and *ant* genes (12). The Mnt and Arc proteins selectively repress *ant* gene expression by binding to two different DNA operator sequences overlapping P_{ant} (13–15). During the early phase of infection, P_{ant} is utilized and a burst of Arc and Ant synthesis results. Arc represses transcription from P_{ant} by binding to an overlapping operator site, O_{arc}. Although Arc also represses its own expression through binding O_{arc}, transcription of *mnt* from P_{mnt} is stimulated, leading to the synthesis of Mnt protein. Mnt binds to O_{mnt} to prevent further expression from P_{ant}, and a stable lysogen can form. In addition, Mnt binding to O_{mnt} activates transcription from P_{mnt} (16).

Repression of *ant* gene expression by Mnt is critical for maintaining the lysogenic state because Ant is able to inactivate c2 repressor function by binding non-covalently to the protein (17). Without functional c2 repressor, lytic gene functions would be fully expressed, and the lytic growth phase would ensue. Although *ant* gene expression does not influence the developmental fate in the wild-type P22 context during normal infection (12), phages that contain an *arc*(Am) mutation dramatically overproduce Ant after infection (13), which can lead to lytic gene functions being expressed. The *arc*(Am)-bacteriophage can form lysogens, however, if transcription of *ant* is prevented. The relative amounts of c2 and Ant proteins synthesized in an infected cell will dictate whether an *arc*(Am)-bacteriophage becomes lysogenic or lytic.

RNA challenge phages are modified versions of P22 in which post-transcriptional regulatory events controlling the expression of *ant* determine the developmental fate of the phage. The modified phage encodes a disruption of *mnt* with a kanamycin resistance gene cassette and an amber mutation within *arc* (Fig. 1b). Sequence-specific RNA-binding activities can be detected using derivatives of P22 that have RNA target sequences substituted for the *ant* 5′-untranslated leader sequence region. The bacteriophage P22$_{R17}$ is a derivative of P22 in which the chosen developmental pathway is regulated by the R17/MS2 coat protein interacting with its RNA target site located in the *ant* mRNA (5). Lysogenic development of the phage relies upon R17/MS2 coat protein expression in the susceptible host cell and the availability of a suitable coat protein binding site encoded by the phage genome. The system was used successfully to identify novel RNA ligands that display reduced affinity for the R17/MS2 coat protein (5) and to select for suppressor coat proteins that recognize mutant RNA ligands (11).

Biological repression specified by generic R17/MS2 RNA operator sites

Recognition of RNA by the R17/MS2 coat protein is specified by a small secondary structure element as shown in Figure 2a. Individual pairs of nucleosides within the helical regions of the structure are not uniquely required for coat protein's RNA-binding activity (Fig. 2b; ref. 18). We assessed whether specific representatives of the consensus RNA ligand structure for coat protein recognition could serve as biological operator sites. RNA challenge phage derivatives were constructed in which the normal *ant* leader sequence region was replaced with different versions of the RNA operator sequence from the R17/MS2 coliphage replicase region (Figs 1c and 2c). The bacteriophage P22$_{R17}$ encodes one version of the consensus RNA operator site. The final basepair that closes the lower helix of the P22$_{R17}$ operator deviates from the natural replicase operator in order to accommodate nucleotide differences found at the second codon for the *ant* open reading frame. The R17/MS2 coat protein directs efficient lysogen formation for P22$_{R17}$ upon coat protein binding to the RNA hairpin within the *ant* mRNA transcript (Fig. 2c; ref. 5). The bacteriophages P22$_{R17}$[L12] and P22$_{R17}$[L14] encode additional variations of the coat protein binding site structure. In these structures the Shine–Dalgarno sequence resides in the 3′ strand of the stem, and the initiation codon for the *ant* gene lies outside the lower helix for each derivative (Fig. 2c). A *S.typhimurium* strain that expresses the coat protein (MS1868[pR17coat(+)]) forms lysogens at a high frequency following infection with either of these two phage derivatives (Fig. 2c). These results reveal that the protein directs translational regulation from RNA operator sites that differ substantially from the natural RNA operator site; however, the data are compatible with the known biochemical properties of the coat protein as a translational repressor (18).

Translational regulation of fragmented RNA operator sites

The consensus coat protein binding site does not require the specific nucleotide pairs within the RNA secondary structure (18). We investigated whether the Shine–Dalgarno sequence could be positioned outside the RNA hairpin bound by the coat protein. The bacteriophages P22$_{R17}$[L19], P22$_{R17}$[L23] and P22$_{R17}$[L28] encode fragmented RNA operator sites, as the coat protein binding determinants within the RNA hairpin do not overlap with the canonical sequences necessary for translation initiation of the Ant open reading frame. These phage derivatives contain the same binding site structure and Shine–Dalgarno sequence 5′ to the *ant* coding sequence. The Shine–Dalgarno sequence lies adjacent to the RNA hairpin in *ant* mRNAs generated from P22$_{R17}$[L19], but is separated from the RNA hairpin in *ant* mRNA transcripts produced from P22$_{R17}$[L23] and P22$_{R17}$[L28] (Fig. 2c). The coat protein causes lysogen formation of P22$_{R17}$[L19] at a frequency of ~40%, nearly twice that observed for P22$_{R17}$ (Fig. 2c). The coat protein induces lysogens at an ~20-fold lower frequency following infection of recipient strains with P22$_{R17}$[L23] (~2% lysogeny). No lysogens were obtained above background levels following infection of recipient cells expressing the coat protein with P22$_{R17}$[L28] (~10^{-6}% lysogeny). The frequencies of lysogeny obtained with P22$_{R17}$[L28] were comparable to phage lacking a translational operator [~10^{-5}% lysogeny with P22*mnt*::Kn9*arc*(Am); Fig. 3].

The results obtained with P22$_{R17}$[L28] were so surprising that we suspected defects in P22$_{R17}$[L28], such as a defective *c2* gene product, might account for the observed low frequency of lysogeny. To test this idea, two additional independent clones of P22$_{R17}$[L28] were constructed and evaluated in lysogen assays using MS1868[pR17coat(+)] as the recipient strain. The results obtained with these two phage clones were identical to the data obtained with the original P22$_{R17}$[L28] (data not shown). Furthermore, the frequency of lysogeny of P22$_{R17}$[L28] was unchanged following phage infection of recipient cells in which coat protein expression was increased by IPTG addition (data not shown). These data strongly imply that the coat protein exerts regulatory control over a discrete portion of the *ant* translational initiation region.

Other bacteriophages employed in these studies yielded unexpected results. The bacteriophage P22$_{R17}$[L18] contains 1 nt of the Shine–Dalgarno sequence within the coat protein binding site; consequently, we anticipated that the coat protein would direct lysogen formation at a frequency between ~1 and ~40%. These values correspond to lysogen frequencies obtained following infection of MS1868[pR17coat(+)] recipient cells with P22$_{R17}$[L14] and P22$_{R17}$[L19], respectively (Fig. 2c). A frequency of only ~2×10^{-5}% lysogeny was obtained following infection of recipient cells with P22$_{R17}$[L18] (Fig. 2c). This result could be explained by the fact that the RNA hairpin from P22$_{R17}$[L18] is predicted to be the least stable of the RNA secondary structures described in this study (19). A bacteriophage derivative that encodes a hybrid RNA hairpin (P22$_{R17}$[L18/19]) was created to yield a more thermodynamically stable secondary structure in which the upper 3 bp of the helix from the RNA hairpin encoded by P22$_{R17}$[L18] were substituted with the corresponding nucleotides from P22$_{R17}$[L19] (Fig. 2c). Lysogen formation occurred at a frequency of 2.1% following infection of recipient cells with the resultant phage P22$_{R17}$[L18/19] (Fig. 2c). This suggests that the failure of coat protein to effectively lysogenize P22$_{R17}$[L18] is attributed to the protein's altered ability to recognize a thermodynamically unstable RNA hairpin rather than to the position of the Shine–Dalgarno sequence within the *ant* mRNA transcript.

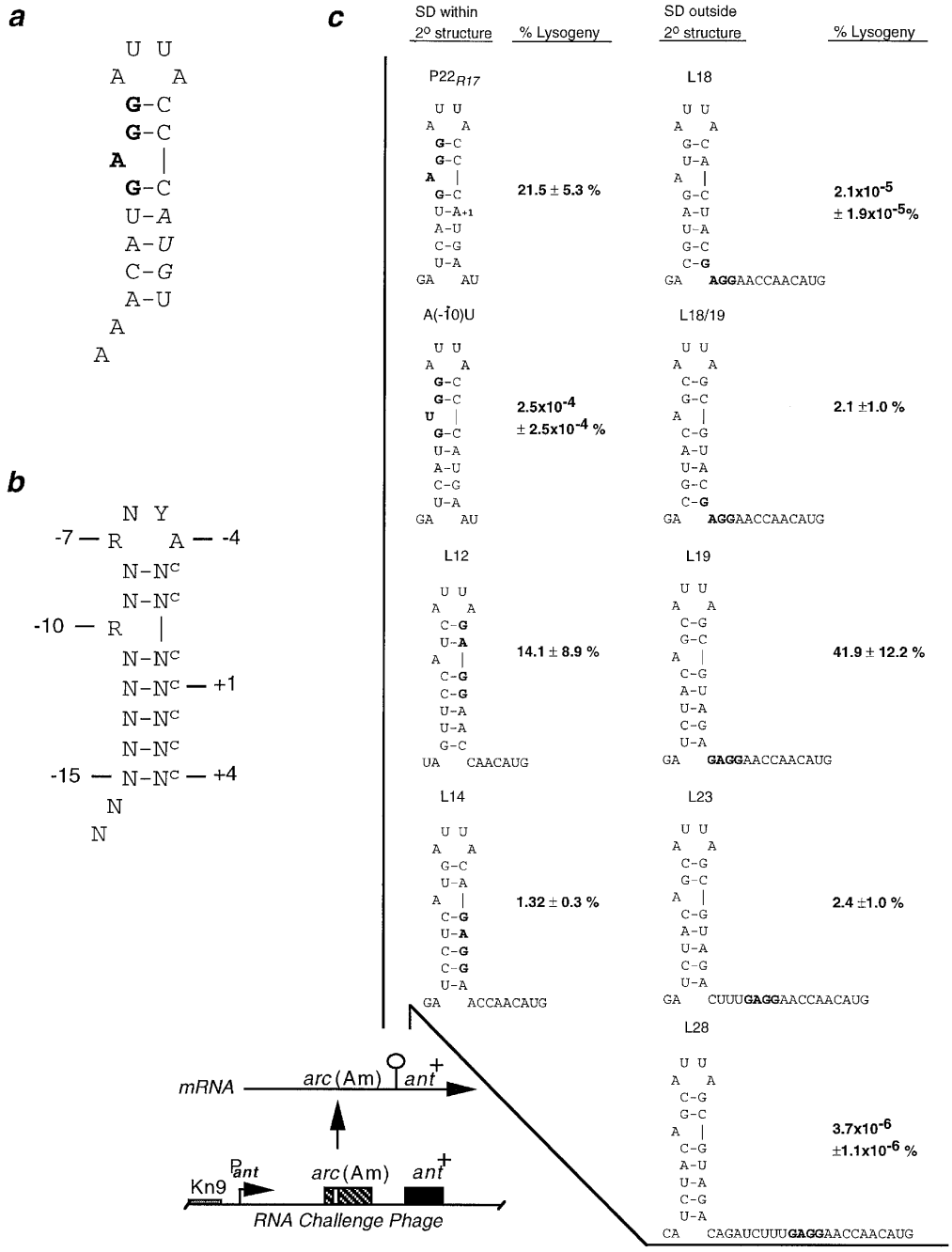

Figure 2. (**a**) Structure of the R17/MS2 coliphage replicase operator site. The Shine–Dalgarno sequence is shown in bold and the initiation codon is illustrated in italics. (**b**) The consensus RNA operator sequence that is bound *in vitro* by the R17/MS2 coat protein. Pyrimidines (Y), purines (R), any nucleotide (N) and its complementary pairing partner (N^C) are indicated (18). (**c**) Lysogen frequency data for RNA challenge phages used in this study with the wild-type coat protein. The predicted RNA secondary structure of the translational operator site and the lysogen frequency data for each derivative following infection of MS1868[pR17coat(+)] are shown. The phages were divided into two groups that was based on the location of the Shine–Dalgarno sequence (denoted as SD) relative to the secondary structure recognized by the coat protein. The standard deviations for the data were calculated from an average of at least three independent infection assays with each bacteriophage where the multiplicity of infection was between 10 and 40.

RNA packaging via encapsidation is a poor means of translational regulation by the R17/MS2 coat protein

Since coat protein dimers bind to the RNA hairpin from $P22_{R17}$[L19], the failure of the wild-type coat protein to effectively lysogenize recipient cells upon infection with $P22_{R17}$[L28] may be due to the coat protein's ability to efficiently assemble into capsid structures lacking *ant* mRNA transcripts. Previously, we obtained genetic and biochemical evidence suggesting that the coat protein forms capsids readily in *S.typhimurium* and at the expense of increased translational repressor capacity *in vivo* (5,11). The coat protein produced from pR17coat(+) is expressed under the control of an IPTG-inducible promoter. Pre-treatment of recipient cells containing this plasmid

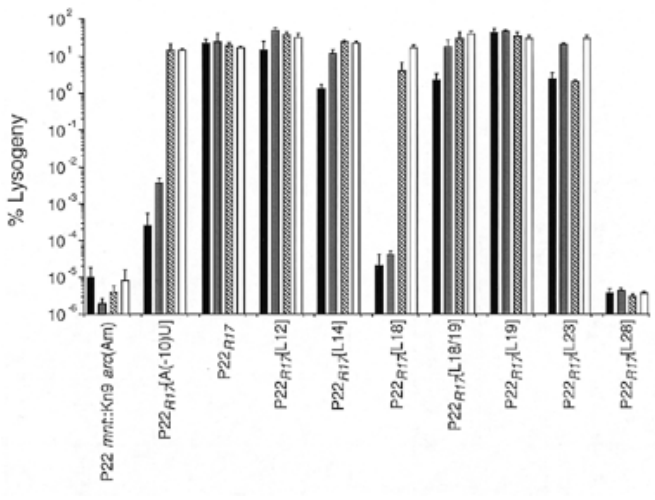

Figure 3. Lysogen frequency data for RNA challenge phages following infection of recipient strains that express R17/MS2 coat proteins with super-repressor activity. MS1868 recipient cells that express either pR17coat(+) (filled columns); pR17coat(+)[N55K] (striped columns); pR17coat(+)[A1D] (shaded columns) or pR17coat(+)[A1D/N55K] (open columns) were infected with each of the indicated bacteriophages as described in Figure 2. The standard deviations for the data were calculated from an average of at least three independent infection assays.

with IPTG results in a 15-fold increase in the steady-state levels of coat protein (11), yet there is no corresponding increase in the frequency of lysogeny following infection by P22$_{R17}$ (5). Our interpretation of these data is that coat protein expression occurs very efficiently from pR17coat(+) without IPTG treatment and that the frequency of lysogeny obtained with P22$_{R17}$ is limited by the intracellular concentration of coat protein dimers that would be available to bind to *ant* mRNA transcripts. An increase in the intracellular concentration of coat protein dimers above the equilibrium constant for capsid formation would result in newly synthesized coat protein being shunted along the pathway leading to capsid structures.

The lysogenic behavior of coat protein mutants with well-defined characteristics was analyzed to determine the features of the coat protein that are responsible for translational regulation. Recently we described two classes of R17/MS2 coat proteins with altered capsid assembly properties and expanded RNA-binding activities (11). One class of these coat protein mutants, exemplified by substitutions such as lysine for asparagine at position 55 in the mature coat protein sequence (N55K), encodes a super-repressor activity toward both wild-type and mutant operator sites (11,20). We tested whether the mutant coat protein [N55K] could direct lysogen formation for several phage derivatives in a fashion similar to that observed by the protein mutant with P22$_{R17}$[A(–10)U] (Fig. 3; ref. 11). Recipient cells harboring pR17coat(+)[N55K] readily survived challenge to lytic infection by P22$_{R17}$[L18] as well as by other phages (P22$_{R17}$[L12], P22$_{R17}$[L14] and P22$_{R17}$[L18/19]; Fig. 3). The mutant protein was able to direct lysogen formation ~3- to ~10^5-fold more effectively than the wild-type coat protein with these phage derivatives (Fig. 3). Both the [N55K] mutant and wild-type coat protein display similar lysogenic properties with the phage series P22$_{R17}$[L19], P22$_{R17}$[L23] and P22$_{R17}$[L28]. The [N55K] mutant can compensate for subtle structural defects in the coat protein binding site; however, the data obtained with the phages encoding fragmented operator sites reveals that the mutant protein either occupies the same area on the *ant* mRNA transcript or forms capsids as efficiently as the wild-type protein (Fig. 3).

A second class of coat protein mutants that were identified in our genetic screen encodes N-terminal substitutions (exemplified by substitutions such as aspartic acid for alanine at position 1 in the mature coat protein) and produces coat proteins defective in capsid assembly (11). Several members of this class have additional defects in post-translational processing of the N-terminal f-Met. We attributed the super-repressor phenotype of the [A1D] mutant to an increase in the intracellular concentration of a coat protein dimer species that recognizes RNA operator sites (Fig. 3; ref. 11). Following infection of recipient cells with phages P22$_{R17}$[L12], P22$_{R17}$[L14] or P22$_{R17}$[L18/19], the coat protein [A1D] mutant directs lysogen formation ~3- to ~10-fold more effectively than the wild-type coat protein (Fig. 3). The [A1D] protein mutant and the wild-type coat protein displayed comparable lysogen frequencies following infection of recipients cells with P22$_{R17}$[L18]. These lysogen frequencies are marginally above the background levels obtained following infection of recipients with a phage lacking an operator site [P22*mnt*::Kn9*arc*(Am); Fig. 3]. The [A1D] protein mutant and the wild-type coat protein direct comparable frequencies of lysogeny with P22$_{R17}$[L19] (~40%) and P22$_{R17}$[L28] (~4 × 10^{-6}%); however, the protein mutant directs lysogen formation ~10-fold more effectively than the wild-type coat protein following infection of recipient cells with P22$_{R17}$[L23] (Fig. 3).

The [A1D] and [N55K] mutants behave quite differently in the RNA challenge phage assays. The [A1D] mutant is a better repressor of P22$_{R17}$[L23]. The [N55K] mutant is more effective with P22$_{R17}$[L14] and P22$_{R17}$[L18] (Fig. 3). The coat protein mutant [A1D/N55K] was recently identified as a novel suppressor of lytic infection by P22$_{R17}$[A(–10)U]. This coat protein mutant embodies both types of amino acid substitutions described above. The new coat protein mutant does not direct lysogen formation in recipient cells following infection by P22$_{R17}$[L28], even though it directs lysogen formation for other phage derivatives that encode an RNA operator site (Fig. 3). The [A1D/N55K] mutant displays properties that are consistent with the mutant's known genotype. Mutants that encode [N55K] and [A1D/N55K] direct comparable lysogen frequencies with recipient cells following infection by P22$_{R17}$[L18]. Mutants that encode [A1D] and [A1D/N55K] display similar frequencies of lysogeny with cells following infection by P22$_{R17}$[L23]. Immunoblot experiments demonstrated that this mixed phenotype cannot be attributed to markedly different levels of protein expression by the [A1D/N55K] mutant gene (Fig. 4a). The [A1D/N55K] mutant does not form native capsids (Fig. 4b), owing to the [A1D] amino acid substitution (11). These results suggest that a specific block in capsid assembly potentiates, rather than attenuates, lysogen formation for phages encoding fragmented operator sites. We conclude that RNA packaging by encapsidation is a poor means of translational regulation by the coat protein.

Ant protein translation occurs efficiently from mRNAs with operator sites

One concern raised by these studies is whether the frequencies of lysogeny displayed by the P22 phage derivatives might be attributed to RNA–RNA interactions or to RNA association with other cellular proteins besides the coat protein. We recently identified an example of an RNA secondary structure differing

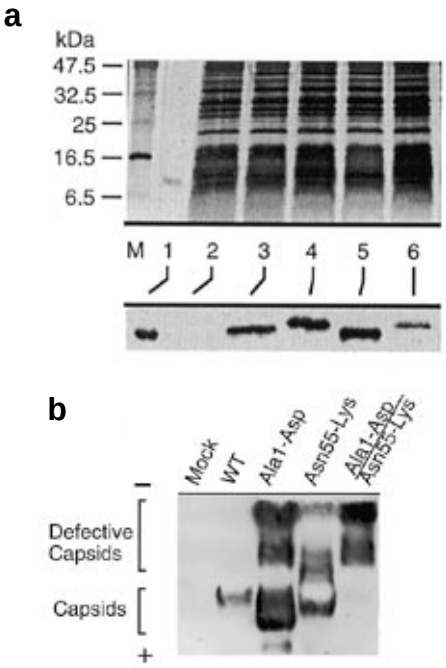

Figure 4. Coat protein expression profiles and capsid assembly. (**a**) Immunoblot analysis of the wild-type coat proteins and mutants expressed *in vivo*. SDS–PAGE of the crude extracts is illustrated in the upper panel; the corresponding immunoblot is shown in the lower panel. Lane M contains the molecular weight standards. Lane 1 contains ~0.5 µg purified R17 coat protein. Lanes 2–6 were loaded with crude extracts prepared from MS1868 strains containing pCKR101 (lane 2), pR17coat(+) (lane 3), Ala1-Asp (lane 4), Asn55-Lys (lane 5) and Ala1-Asp/Asn55-Lys (lane 6) following induction with IPTG to a final concentration of 1 mM. Each lane (2–6) contains 5 µg of total protein. (**b**) *In vivo* assembly assay of capsid formation for coat protein mutants. The lanes designated as Mock and WT contain clarified cell lysate prepared from MS1868 and MS1868[pR17coat(+)], respectively. The MS1868 lysates that express each coat protein mutant are denoted above each lane. The anode (+) and cathode (–) electrodes are shown to indicate the direction of electrophoresis. The positions where intact capsids and defective structures migrate in the agarose gel are shown.

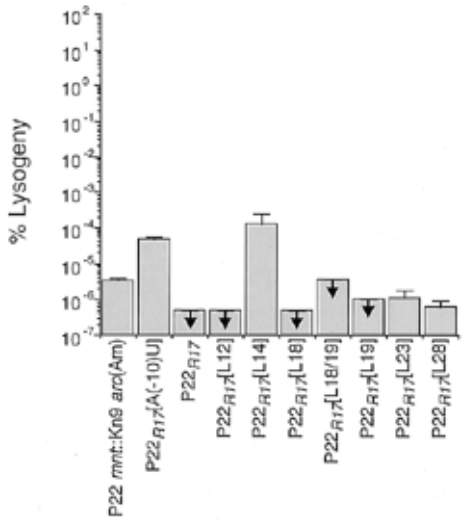

Figure 5. Lysogen frequencies for bacteriophages in MS1868 recipient cells. Cases in which the lysogen frequency was below the limits of detection for the dilution series analyzed in plating experiments are indicated by downward arrows. The standard deviations for the data were calculated from an average of at least three independent infection assays.

from those described in this work that moderates lysogen development for another P22 phage derivative, presumably by affecting Ant protein translation (manuscript in preparation). All the phage derivatives described herein were initially identified and selected by their ability to form clear plaques on MS1883, indicating that the encoded RNA secondary structure does not interfere with Ant protein translation. We also evaluated the frequencies of lysogeny for these phages following infection of MS1868 recipient cells that lack coat protein expression. None of these phages forms lysogens at frequencies substantially above background infection of this recipient strain with P22*mnt*::Kn9*arc*(Am), a phage derivative lacking an operator site (Fig. 5). We conclude that each of the constructed phage derivatives encode a translational initiation region whose secondary structure can be unfolded for the initiation of Ant protein biosynthesis.

DISCUSSION

The R17/MS2 coat protein binds to an RNA secondary structure with few specific nucleotide requirements. The primary sequence determinants include a well-conserved adenosine located within the structure of the loop sequence at position –4 (A_{-4}; ref. 21), a purine at position –7 (18), and a bulged purine at position –10 relative to the first nucleotide of the replicase initiation codon (22,23). The remaining nucleotide identities within the loop and in the stem are not critical for coat protein binding so long as the secondary structure is preserved (21,23), although the nucleotide at position –5 modulates coat protein binding affinity (24). The crystal structure of an operator RNA fragment with coat protein dimer in the context of the phage capsid has been solved and it provides a rationalization for many of these sequence determinants (25).

The primary sequence determinants necessary for coat protein binding have enabled assessment of substituted generic operator sites for the natural operator sequence. Our results with several phage derivatives indicate that the coat protein can regulate translation of an artificial RNA operator site that provides the native secondary structure of the RNA hairpin. Mutant coat proteins that possess enhanced RNA-binding activity can suppress some defects in the RNA hairpin structure such as those manifested in *ant* mRNA transcripts encoded by P22$_{R17}$[L18] and P22$_{R17}$[A(–10)U]. Several other RNA hairpins that are bound efficiently by the coat protein *in vitro* lack an adequate Shine–Dalgarno sequence (26); therefore, these RNA structures could not be evaluated in the RNA challenge phage system.

Translational regulation by the coat protein can be effectively accomplished for mRNA transcripts in which the Shine–Dalgarno sequence is removed entirely from the RNA secondary structure recognized by the protein. The extent to which the Shine–Dalgarno sequence can be positioned away from the RNA hairpin is limited. The wild-type coat protein behaves as a poor translational repressor of *ant* mRNA transcripts when the distance separating these two genetic elements is 4 or 9 nt. Coat protein mutants with a compromised ability to form native capsid structures recognize and repress several RNA operator sites that are not normally subject to translational regulation by the wild-type protein [e.g., A(–10)U; ref. 5]. The RNA-binding activity of these mutant proteins may be attributed to an increase in the intracellular concentration of dimer

species or to subtle differences in the manner whereby the mutant protein dimer species interacts with the RNA hairpin.

Our data with the phages encoding the fragmented RNA operator sites allows us to expand our understanding of how a translational repressor functions and to discriminate between various models of translational repression. Appropriate regulation of translation is retained for RNA operators in which the Shine–Dalgarno sequence is placed entirely outside the coat protein binding site; therefore, we discount the importance of any model that stipulates that the Shine–Dalgarno sequence must be sequestered within a stable RNA secondary structure for translational repression. The occlusion model is difficult to reconcile when one considers all the data obtained with this system. The structural information gleaned from the crystallographic and solution data for the RNA–coat protein complex (25,27) provide several constraints on the manner in which the coat protein interacts with the RNA hairpin. The coat protein dimer within the capsid establishes asymmetric contacts with its RNA ligand. Most of the RNA–protein contacts reside on the 5′ side of the RNA secondary structure with A_{-4} being the furthest 3′ contact with the coat protein dimer (25). The RNA challenge phage data indicate that the wild-type coat protein is only marginally effective at repressing translation when the Shine–Dalgarno element is positioned ≥11 nt 3′ to this conserved adenosine. The possibility that a coat protein dimer can physically mask the Shine–Dalgarno sequence on these mRNAs is unlikely, unless the coat protein assembles a higher order structure on the *ant* mRNA transcripts from P22$_{R17}$[L19] and P22$_{R17}$[L23].

Our bacteriophage data can be rationalized with a model in which a coat protein-stabilized RNA secondary structure contributes to translational regulation. Stabilization energy is provided to the RNA secondary structure by the binding of the coat protein (28). The ribosome encounter site is experimentally defined as a region –17 to +16 on the mRNA transcript (29). Nucleotides at positions –16 and –17 lie within the RNA hairpin for *ant* mRNA transcripts encoded by P22$_{R17}$[L23]. Sequence determinants within the translational initiation region through nucleotide –20 lie 3′ of the RNA hairpin for P22$_{R17}$[L28], the only phage that was not lysogenized by recipient strains that express the coat protein. The coat protein exerts translational regulation by precluding access of ribosomal components on the mRNA transcript, including additional determinants within the stem region of the operator site other than the Shine–Dalgarno sequence and the initiation codon (Fig. 6).

In addition to its role as a translational repressor of replicase, the coat protein packages phage genomic RNA. The RNA operator site was originally thought to be the principal site where the packaging reaction initiates during natural infection since one coat protein dimer would bind to this site on the RNA genome midway through the replication cycle (18). The P22$_{R17}$[L28] phage did not form lysogens in any recipient strains that expressed either the wild-type coat protein or one of the super-repressor coat proteins. Ant protein synthesis can occur during infection because the coat protein dimer and ribosome components are presumed to bind to adjacent sites on the *ant* mRNA transcript from P22$_{R17}$[L28]. Lysogen formation should result for all phages that contain an RNA operator site at any location within the *ant* mRNA transcript if RNA encapsidation occurs. The low frequency of lysogeny data obtained with P22$_{R17}$[L28] indicates that RNA encapsidation is not a plausible means of translational regulation. The coat protein can efficiently

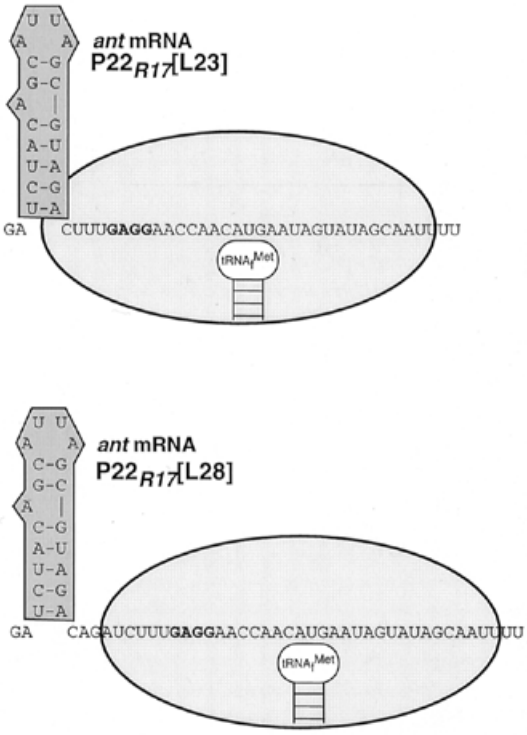

Figure 6. Protein-stabilized RNA folding prevents translation for an artificial operator site. The coat protein can exert regulatory influence on a translational initiation region as long as the linear sequence determinants necessary for ribosome recognition and binding are contained within the RNA secondary structure (denoted here as the overlapping region in the *ant* mRNA transcript encoded by P22$_{R17}$[L23]).

package genomic RNA that lacks an adequate RNA operator site (7) and other large heterologous RNAs into capsids (7,30), suggesting that the RNA operator is not an essential *cis*-acting determinant of RNA packaging. A key determinant of RNA packaging undoubtedly includes an RNA substrate devoid of ribosomes. The translationally repressive nature of RNA secondary structure alone would provide such an RNA substrate (31–35) and probably contributes significantly to the selectivity of genomic RNA packaging during a natural infection cycle for the R17/MS2 coliphage.

The occupancy of the translational initiation region by a repressor protein to prevent binary complex formation is not limited to the R17/MS2 coat protein; this mechanism represents a common mode of translational regulation in prokaryotic phage and host cell proteins. The bacteriophage T4 regA protein represses translation of a number of early T4 mRNAs (36). RegA binds specifically to a single-stranded RNA sequence located in the translational initiation region (1,4). The protein occupies the region encompassing the Shine–Dalgarno sequence and part of the initiation codon for the gene 44 mRNA (37) and binds to the RNA region that includes the initiation codon for the rIIB gene mRNA (38). The T4 DNA polymerase binds to a stem–loop structure located 5′ to the Shine–Dalgarno sequence and occupies the region extending from the initial RNA-binding site to near the initiation codon (39). The T4 gene 32 protein initially binds to a pseudoknot structure located 5′ to the Shine–Dalgarno sequence, and then multimerizes along the RNA until it physically masks the

Shine–Dalgarno sequence (40). The threonyl-tRNA synthetase binds to a tRNA-like clover-leaf structure located 5′ of the Shine–Dalgarno sequence for the gene encoding *thr*S, thereby controlling its own synthesis (41,42). These diverse biological operators function according to a common mechanism and one that is shared with the R17/MS2 coat protein. Similar flexibility in operator structure might also exist for the function of these translational regulatory systems.

The translational repressor system of the R17/MS2 coliphage provides an elegant example of the compromise struck in a natural RNA operator site in balancing the requirement of the RNA secondary structure for regulatory protein binding with the need for ribosome access to linear sequence determinants. The study of the artificial RNA operator sites described in this work not only reveals new insights about the manner in which a translational repressor exerts regulatory control over its mRNA substrate but highlights how RNA-binding proteins may regulate the folded structure of RNA and its function. In the example reported here, translational regulation was modulated by the folded state of an RNA ligand bound by a protein. The extensive region required for translational initiation in bacterial mRNA transcripts offers a rich playground in which numerous types of interacting RNA and protein molecules can affect translation. The full measure of the diversity of translational control remains to be explored.

ACKNOWLEDGEMENTS

We thank E.M.Seitz and K.A.Bennett for excellent technical assistance, O.C.Uhlenbeck who provided encouragement for initial aspects of this work, and D.S.Peabody for discussion. This work was supported by NIH grant GM47854.

REFERENCES

1 Gold,L. (1988) *Annu. Rev. Biochem.* **57**, 199–233.
2 Bernardi,A. and Spahr,P.F. (1972) *Proc. Natl. Acad. Sci. USA* **69**, 3033–3037.
3 Draper,D.E. (1993) in Nierhaus,K.H., Franceschi,F., Subramanian,A.R., Erdmann,V.A. and Wittmann-Liebold,B. (eds), *The Translational Apparatus.* Plenum Press, New York, pp. 197–207.
4 McCarthy,J.E.G. and Gualerzi,C. (1990) *Trends Genet.* **6**, 78–85.
5 MacWilliams,M.P., Celander,D.W. and Gardner,J.F. (1993) *Nucleic Acids Res.* **21**, 5754–5760.
6 Pickett,G.G. and Peabody,D.S. (1993) *Nucleic Acids Res.* **21**, 4621–4626.
7 Peabody,D.S. (1997) *Mol. Gen. Genet.* **254**, 358–364.
8 Fouts,D.E. and Celander,D.W. (1996) *Nucleic Acids Res.* **24**, 1582–1584.
9 Kunkel,T.A., Bebenek,K. and McClary,J. (1991) *Methods Enzymol.* **204**, 125–139.
10 Sears,L.E., Moran,L.S., Kissinger,C., Creasey,T., Perry-O'Keefe,H., Roskey,M., Sutherland,E. and Slatko,B.E. (1992) *BioTechniques* **13**, 626–633.
11 Wang,S., True,H.L., Seitz,E.M., Benett,K.A., Fouts,D.E., Gardner,J.F. and Celander,D.W. (1997) *Nucleic Acids Res.* **25**, 1649–1657.
12 Susskind,M. and Youderian,P. (1983) in Hendrix,R.W., Roberts,J.W., Stahl,F.W. and Weisberg,R.A. (eds), *Lambda II.* Cold Spring Harbor University Press, Cold Spring Harbor, NY, pp. 347–363.
13 Susskind,M.M. (1980) *J. Mol. Biol.* **138**, 685–713.
14 Vershon,A.K., Youderian,P., Susskind,M.M. and Sauer,R.T. (1985) *J. Biol. Chem.* **260**, 12124–12129.
15 Sauer,R.T., Krovatin,W., DeAnda,J., Youderian,P. and Susskind,M.M. (1983) *J. Mol. Biol.* **168**, 699–713.
16 Vershon,A.K., Liao,S.-M., McClure,W.R. and Sauer,R.T. (1987) *J. Mol. Biol.* **195**, 311–322.
17 Susskind,M.M. and Botstein,D. (1975) *J. Mol. Biol.* **98**, 413–424.
18 Witherell,G.W., Gott,J.M. and Uhlenbeck,O.C. (1991) *Prog. Nucleic Acid Res. Mol. Biol.* **40**, 185–220.
19 Serra,M.J. and Turner,D.H. (1995) *Methods Enzymol.* **259**, 242–261.
20 Lim,F., Spingola,M. and Peabody,D.S. (1994) *J. Biol. Chem.* **269**, 9006–9010.
21 Carey,J., Lowary,P.T. and Uhlenbeck,O.C. (1983) *Biochemistry* **22**, 4723–4730.
22 Wu,H.-N. and Uhlenbeck,O.C. (1987) *Biochemistry* **26**, 8221–8227.
23 Romaniuk,P.J., Lowary,P., Wu,H.-N., Stormo,G. and Uhlenbeck,O.C. (1987) *Biochemistry* **26**, 1563–1568.
24 Lowary,P.T. and Uhlenbeck,O.C. (1987) *Nucleic Acids Res.* **15**, 10483–10493.
25 Valegård,K, Murray,J.B., Stockley,P.G., Stonehouse,N.J. and Liljas,L. (1994) *Nature* **371**, 623–626.
26 Schneider,D., Tuerk,C. and Gold,L. (1992) *J. Mol. Biol.* **228**, 862–869.
27 Carey,J., Cameron,V., deHaseth,P.L. and Uhlenbeck,O.C. (1983) *Biochemistry* **22**, 2601–2610.
28 Carey,J. and Uhlenbeck,O.C. (1983) *Biochemistry* **22**, 2610–2615.
29 Steitz,J.A. (1969) *Nature* **224**, 957–964.
30 Beckett,D., Wu,H.N. and Uhlenbeck,O.C. (1988) *J. Mol. Biol.* **204**, 939–947.
31 Berkhout,B., Schmidt,B.F., van Strien,A., van Boom,J., van Westrenen,J. and van Duin,J. (1987) *J. Mol. Biol.* **195**, 517–524.
32 Berkhout,B. and van Duin,J. (1985) *Nucleic Acids Res.* **13**, 6955–6967.
33 Eggen,K., Oeschger,M.P. and Nathans,D. (1967) *Biochem. Biophys. Res. Commun.* **28**, 587–597.
34 Hindley,J. and Staples,D.H. (1969) *Nature* **224**, 964–967.
35 Min Jou,W., Haegeman,G., Ysebaert,M. and Fiers,W. (1972) *Nature* **237**, 82–88.
36 Wiberg,J.S. and Karam,J.D. (1983) in Mathews,C.K., Kutter,E.M., Mosig,G. and Berget,P.B. (eds), *Bacteriophage T4.* American Society for Microbiology, Washington, DC, pp. 193–201.
37 Webster,K.R., Adari,H.Y. and Spicer,E.K. (1989) *Nucleic Acids Res.* **17**, 10047–10068.
38 Winter,R.B., Morrissey,L., Gauss,P., Gold,L., Hsu,T. and Karam,J. (1987) *Proc. Natl. Acad. Sci. USA* **84**, 7822–7826.
39 Andrake,M., Guild,N. Hsu,T., Gold,L., Tuerk,C. and Karam,J. (1988) *Proc. Natl. Acad. Sci. USA* **85**, 7942–7946.
40 McPheeters,D.S., Stormo,G.D. and Gold,L. (1988) *J. Mol. Biol.* **201**, 517–535.
41 Springer,M., Plumbridge,J.A., Butler,J.S., Graffe,M., Dondon,J., Mayaux,J.F., Fayat,G., Lestienne,P., Blanquet,S. and Grunberg-Manago,M. (1985) *J. Mol. Biol.* **185**, 93–104.
42 Moine,H., Romby,P., Springer,M., Grunberg-Manago,M., Ebel,J.P., Ehresmann,C. and Ehresmann,B. (1988) *Proc. Natl. Acad. Sci. USA* **85**, 7892–7896.
43 Bullock,W.O., Fernandez,J.M. and Short,J.M. (1987) *BioTechniques* **5**, 376–379.